Dynamics of Glomerular Ultrafiltration in the Rat

IV. DETERMINATION OF THE ULTRAFILTRATION COEFFICIENT

WILLIAM M. DEEN, JULIA L. TROY, CHANNING R. ROBERTSON, and BARRY M. BRENNER

From the Departments of Medicine, Veterans Administration Hospital, San Francisco, California 94121, and the University of California, San Francisco, California 94122, and the Department of Chemical Engineering, Stanford University, Stanford, California 94305

ABSTRACT Pressures and flow rates were measured in accessible surface glomeruli of mutant Wistar rats under conditions deliberately designed to prevent achievement of filtration pressure equilibrium, that is, the equalization of transcapillary hydrostatic and oncotic pressures by the efferent end of the glomerulus as typically observed in the normal hydropenic rat. Disequilibrium was obtained at elevated levels of glomerular plasma flow (GPF) brought about by acute expansion of plasma volume with a volume of rat plasma equal to 5% of body weight. Glomerular hydrostatic and oncotic pressures measured at high GPF were used to calculate the ultrafiltration coefficient, K_f, the product of effective hydraulic permeability and surface area. GPF was then either lowered (by aortic constriction) or raised (by carotid occlusion) in order to examine the dependence of K_f on GPF. The value of K_f per glomerulus, 0.08 nl/(s·mm Hg), was found not to vary over an approximately twofold range of GPF. This finding, taken together with data from previous studies from this laboratory, leads us to conclude that plasma-flow dependence of glomerular filtration rate (GFR) results primarily from flow-induced changes in mean ultrafiltration pressure, rather than large changes in K_f.

INTRODUCTION

Glomerular ultrafiltration, as with fluid movement across other capillary membranes, is governed by the imbalance of transcapillary hydrostatic and osmotic pressure differences. At any point along a glomerular capillary the net driving force (P_{UF}) is given by

$$P_{UF} = \Delta P - \Delta\pi = (P_{GC} - P_T) - (\pi_{GC} - \pi_T) \quad (1)$$

where P_{GC} and P_T are the hydrostatic pressures in the glomerular capillary and proximal tubule, respectively, and π_{GC} and π_T are the corresponding colloid osmotic pressures. Since tubule fluid is essentially protein-free, π_T is negligible and $\Delta\pi = \pi_{GC}$.

The rate of glomerular ultrafiltration may be expressed as

$$\text{SNGFR} = K_f \cdot \bar{P}_{UF} = k \cdot S \cdot \bar{P}_{UF} \quad (2)$$

where SNGFR is the single nephron glomerular filtration rate, $\bar{P}_{UF}$ is the mean driving pressure (P_{UF} averaged along the length of the capillary), and K_f, the ultrafiltration coefficient, is the product of the effective hydraulic permeability (k) and surface area (S) of the glomerular capillaries. As indicated by equation 2, K_f must be characterized before SNGFR can be analyzed in terms of the responsible hydrostatic and osmotic pressures. Recent micropuncture studies from this laboratory (1, 2) have demonstrated a high degree of plasma-flow dependence of SNGFR in the rat. Remaining to be determined are the relative contributions of changes in K_f and P_{UF} to the observed flow dependence of SNGFR.

The use of servo-nulling pressure transducers and microanalytical protein assay methods in rats with surface glomeruli has made it possible to directly

Dr. Brenner is a Medical Investigator of the Veterans Administration.

Received for publication 20 November 1972 and in revised form 2 February 1973.

measure $\bar{P}_{GC}$[1] and P_T and to determine colloid osmotic pressure in afferent (π_{AA}) and efferent (π_{EA}) arteriolar plasma (1–3). Provided that $\bar{P}_{UF}$ could be evaluated from these pressure measurements, equation 2 would allow calculation of K_f from measurements of $\bar{P}_{UF}$ and SNGFR. However, under conditions of filtration pressure equilibrium, the near equality of ΔP and $\Delta\pi$ normally existing at the efferent end of the glomerular capillary (1–4), it is impossible to estimate $\bar{P}_{UF}$, and thus K_f, due to the uncertainty in determining $\bar{\pi}_{GC}$. This uncertainty results from the fact that since the local rate of ultrafiltration is proportional to P_{UF}, π_{GC} will increase most rapidly at the afferent end of the capillary. As discussed in detail elsewhere (5), filtration pressure equilibrium requires that the profile of π_{GC} along a capillary be highly nonlinear, and allows for any number of nonlinear profiles to correspond to given measurements of π_{AA} and π_{EA} (5). Curves 1 and 2 in Fig. 1 show two possible profiles. For a given initial glomerular plasma flow rate (GPF), curve 1 corresponds to a larger value of K_f than does curve 2. Generally speaking, an increase in K_f above the minimum value required to yield equilibrium results in a more rapid approach to equilibrium (as in curve 1) but essentially the same final value of $\Delta\pi$, measured as π_{EA}. Since $\bar{P}_{UF}$ is equal to the area between the ΔP and $\Delta\pi$ curves as plotted in Fig. 1, $\bar{P}_{UF}$ and therefore K_f cannot be uniquely determined from the available measurements at equilibrium. Under these conditions, assumption of a linear $\Delta\pi$ profile, $\bar{\pi}_{GC} = (\pi_{AA} + \pi_{EA})/2$, yields a unique but not very meaningful estimate of $\bar{P}_{UF}$, since it excludes the possibility of $\bar{P}_{UF}$ changing as the result of flow-induced changes in the $\Delta\pi$ profile (5).

The goal of the present study was to achieve disequilibrium conditions in the rat, thereby allowing K_f to be calculated from the measured values of $\bar{P}_{GC}$, P_T, π_{AA}, π_{EA}, and GPF according to a recently developed model of glomerular ultrafiltration (5). This was accomplished by means of acute expansion of plasma volume by intravenous infusion of homologous rat plasma equal to 5% of body weight, which has the effect of markedly elevating GPF. After completion of measurements needed to calculate K_f under this condition, GPF was then either increased further (by carotid occlusion) or decreased (by aortic constriction) to determine whether K_f varies with GPF. The results indicate that K_f is remarkably insensitive to wide variations in GPF.

[1] The values for P_{GC} reported in the present study represent time averages. Peak to valley amplitudes of single glomerular capillary pressure pulses average approximately 8 mm Hg and bracket these time averaged values equally during systole and diastole. The term $\bar{P}_{GC}$ represents P_{GC} averaged over the length of the glomerular capillary, the justification for which has been discussed previously (1).

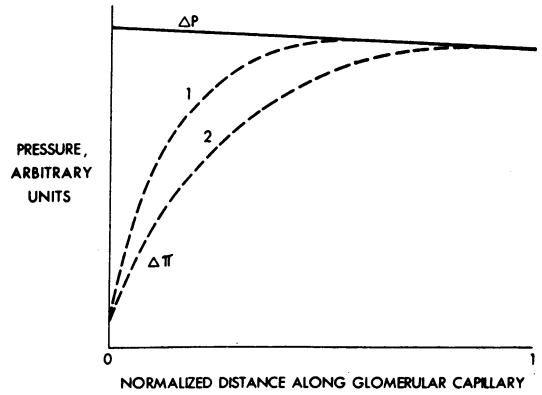

FIGURE 1 Hydrostatic and osmotic pressure profiles along an idealized glomerular capillary. $\Delta P = P_{GC} - P_T$ and $\Delta\pi = \pi_{GC} - \pi_T$.

GLOSSARY OF SYMBOLS

a_1, a_2	Empirical constants, mm Hg/(g/100 ml) and mm Hg/(g/100 ml)^2, respectively.
A_1, A_2	Dimensionless osmotic pressure coefficients, equations 16 and 17.
AABF, AAPF	Afferent arteriolar blood flow and plasma flow, respectively, nl/min.
$\overline{AP}$	Mean femoral arterial pressure, mm Hg.
C	Protein concentration, g/100 ml.
C^*	Dimensionless protein concentration, C/C_{AA}.
EABF, EAPF	Efferent arteriolar blood flow and plasma flow, respectively, nl/min.
F	Permeability and plasma flow rate parameter. equation 15.
GBF, GPF	Glomerular blood flow and plasma flow, respectively, nl/min.
Hct_{AA}	Blood hematocrit in femoral artery or afferent arteriole.
I	Integration constant in equation 18.
k	Effective hydraulic permeability, nl/(s·mm Hg·cm^2) or nl/(min·mm Hg·cm^2).
K_f	Ultrafiltration coefficient, equation 2, nl/(s·mm Hg) or nl/(min·mm Hg).
P	Hydrostatic pressure, mm Hg.
P_{UF}	Net ultrafiltration pressure, equation 1, mm Hg.
ΔP	Transmembrane hydrostatic pressure difference, $P_{GC} - P_T$, mm Hg.
π	Colloid osmotic pressure, mm Hg.
$\Delta\pi$	Transmembrane osmotic pressure difference, $\pi_{GC} - \pi_T$, mm Hg.
R	Resistance to blood flow, dyn·s·cm^{-5}.
R_{TA}	Total arteriolar resistance, $R_A + R_E$, dyn·s·cm^{-5}.
S	Surface area available for ultrafiltration, cm^2.
SNFF	Single nephron filtration fraction.
SNGFR	Single nephron glomerular filtration rate, nl/min.
$(TF/P)_{IN}$	Tubule fluid to plasma inulin concentration ratio.
V_{TF}	Tubule fluid flow rate, nl/min.
x	Distance along capillary from point at which filtration begins, cm.
x^*	Dimensionless distance along capillary.

SUPERSCRIPTS

—	Mean value.
*	Dimensionless variable.

SUBSCRIPTS

A or *AA*	Afferent arteriole.
C	Peritubular capillary.
E or *EA*	Efferent arteriole.
GC	Glomerular capillary.
T	Proximal tubule.

METHODS

Experiments were performed in 22 adult mutant Wistar rats weighing 180–310 g. and allowed free access to food and water before study. Rats were anesthetized with Inactin (100 mg/kg) and prepared for micropuncture as described previously (6–8). Before study all rats underwent isoncotic plasma expansion, receiving intravenous infusion of a volume of homologous rat plasma (obtained by arterial exsanguination of a littermate on the morning of study) equal to 5% body weight, administered in a 90 min period beginning 120 min before micropuncture. 60 min before micropuncture rats received an intravenous infusion of isotonic NaCl at the rate of 0.02 ml/min. Inulin was present in a concentration of 10%, thereby resulting in final plasma concentration of about 100 mg/100 ml. Mean femoral arterial pressure ($\overline{AP}$) was monitored by means of an electronic transducer (model P23AA, Statham Instruments, Inc., Oxnard, Calif.) connected to a direct-writing recorder (model 7702B, Hewlett-Packard Co., Palo Alto, Calif.). Late surface convolutions of proximal tubules were identified as described previously (6–8). After this 60 min equilibration period, exactly timed (1–2 min) samples of fluid were collected from each experimental tubule for determination of flow rate and inulin concentration, and calculation of SNGFR. The rate of fluid collection was adjusted to maintain a column of polymer oil (Kel F polymer oil, 3M Co., Medical Products Div., St. Paul, Minn.), three to four tubule diameters in length, in a relatively constant position just distal to the site of puncture. Using the collection technique of controlled suction recently validated for this laboratory (9), minimal changes in tubule diameter or the position of the distal oil block were produced. Coincident with these tubule fluid collections, femoral arterial blood samples were obtained for determinations of hematocrit and plasma inulin concentration.

Hydrostatic pressures were measured in single glomerular capillaries within surface glomeruli using continuous recording, servo-nulling micropipette transducer techniques (8, 10, 11). Micropipettes with outer tip diameters of 2–3 μm and containing 1.0 M NaCl were used. Penetration of Bowman's capsule and entry into capillaries was performed under stereomicroscopic control. Hydraulic output from the servo-system was channeled via a transducer (Statham Instruments, Inc., P23Db) to a second channel of the recorder. Accuracy, frequency response and stability features of this servo-system have been described in detail elsewhere (8). In addition to direct measurements of glomerular capillary hydrostatic pressure (P_{GC}), and proximal tubule pressure (P_T), pressures also were recorded in efferent arterioles (P_{EA}) and second- and third-order branch peritubular capillaries (P_C) in each rat.

To obtain estimates of colloid osmotic pressure (π) of plasma entering and leaving glomerular capillaries, protein concentrations in femoral arterial and efferent arteriolar blood plasmas were measured as described previously (6). Colloid osmotic pressures were calculated from the equation for plasma derived by Landis and Pappenheimer (12) and recently validated for the rat (13). π calculated for femoral arterial plasma will be taken as representative of π for the afferent arteriole (π_{AA}). These estimates of pre- and postglomerular protein concentration permit calculation of single nephron filtration fraction (SNFF), and GPF (see equations below). From direct measurements of the decline in pressure along single afferent and efferent arterioles, and estimates of blood flow through these vessels, vascular resistances to blood flow through these individual vessels were calculated (see equations 9–11).

After completion of the above measurements, we induced reductions in GPF in nine rats by means of partial constriction of the abdominal aorta. This reduction in perfusion pressure to the left (experimental) kidney was achieved by applying tension to a fine silk ligature encircling the abdominal aorta between the origins of the renal arteries (14). Many or all of the above determinations of SNGFR (using the recollection micropuncture technique), SNFF, GPF, glomerular transcapillary hydrostatic ($\bar{P}_{GC}$, P_T) and oncotic pressure (π_{EA}, π_{AA}) and vascular resistances were repeated at the reduced renal perfusion pressure in each rat. The period of time required to obtain all of the measurements and collections was usually less than 30 min for each level of $\overline{AP}$.

In eight plasma loaded rats, after initial measurements of glomerular pressures and flows, GPF was further increased by means of occlusion of both common carotid arteries together with bilateral cervical vagotomy. Measurements of the necessary quantities were then repeated in the ensuing 30 min interval, with the recollection micropuncture technique used for the repeat determination of SNGFR.

Analytical. The volume of tubule fluid collected from individual nephrons was estimated from the length of the fluid column in a constant bore capillary tube of known internal diameter. The concentration of inulin in tubule fluid was measured, usually in duplicate, by the microfluorescence method of Vurek and Pegram (15). Inulin concentration in plasma was determined by the macroanthrone method of Führ, Kaczmarczyk and Krüttgen (16). Protein concentrations in efferent arteriolar and femoral arterial blood plasmas were determined, usually in duplicate, with an ultramicro-colorimeter[2] using a recently described (6) microadaptation of the method of Lowry, Rosebrough, Farr, and Randall (17).

Calculations. Single nephron glomerular filtration rate:

$$\text{SNGFR} = (\text{TF/P})_{IN} \cdot V_{TF} \qquad (3)$$

where $(\text{TF/P})_{IN}$ and V_{TF} refer to transtubular inulin concentration ratio and tubule fluid flow rate, respectively.

Single nephron filtration fraction:

$$\text{SNFF} = 1 - \frac{C_{AA}}{C_{EA}} \qquad (4)$$

[2] Designed and constructed by Dr. Gerald Vurek, Laboratory of Technical Development, National Heart and Lung Institute, Bethesda, Md.

where C_{AA} and C_{EA} denote afferent and efferent arteriolar protein concentrations, respectively.

Plasma flow rate per single afferent arteriole (AAPF) and therefore, the initial plasma flow rate per glomerulus (GPF):

$$\text{AAPF} = \text{GPF} = \frac{\text{SNGFR}}{\text{SNFF}} \tag{5}$$

Blood flow rate per single afferent arteriole or glomerulus:

$$\text{AABF} = \text{GBF} = \text{AAPF} \cdot \left(\frac{1}{1 - \text{Hct}_{AA}} \right) \tag{6}$$

where Hct_{AA}, the hematocrit of afferent arteriolar blood, is taken as equal to the hematocrit value for femoral arterial blood.

Plasma flow per efferent arteriole:

$$\text{EAPF} = \text{GPF} - \text{SNGFR} \tag{7}$$

Blood flow rate per efferent arteriole:

$$\text{EABF} = \text{GBF} - \text{SNGFR} \tag{8}$$

Resistance per single afferent arteriole:

$$R_A = \frac{\overline{AP} - \bar{P}_{GC}}{\text{GBF}} \times (7.962 \times 10^{10}) \tag{9}$$

where the factor 7.962×10^{10} is used to give resistance in units of dyn·s·cm^{-5} when $\overline{AP}$ and $\bar{P}_{GC}$ are expressed in mm Hg and GBF in nanoliters per minute.

Resistance per single efferent arteriole:

$$R_E = \frac{\bar{P}_{GC} - P_C}{\text{EABF}} \times (7.962 \times 10^{10}) \tag{10}$$

Total arteriolar resistance for a single pre- to postglomerular vascular unit:

$$R_{TA} = R_A + R_E \tag{11}$$

An estimate of the net ultrafiltration pressure at the afferent end of the glomerular capillary ($P_{UF_{AA}}$) is given by the expression:[3]

$$P_{UF_{AA}} = \bar{P}_{GC} - P_T - \pi_{AA} \tag{12}$$

An estimate of the net ultrafiltration pressure at the efferent end of the glomerular capillary ($P_{UF_{EA}}$) is given by the equation:[3]

$$P_{UF_{EA}} = \bar{P}_{GC} - P_T - \pi_{EA} \tag{13}$$

The ultrafiltration coefficient (K_f) is calculated using a differential equation which gives the rate of change of protein concentration (C) with distance (x) along an idealized glomerular capillary. The derivation of this equation, described in detail elsewhere (5), treats the glomerular capillary bed as a rigid cylindrical tube of equivalent total surface area, impermeable to plasma proteins, and with plasma flow rate and C dependent only on the axial coordinate x. The net transcapillary driving force (P_{UF}) is given by equation 1. Since ΔP has been found to decline by no more than a small amount along the glomerular capillary (1), the nondimensional form of the differential equation can be reduced to

$$\frac{dC^*}{dx^*} = FC^{*2}(1 - A_1C^* - A_2C^{*2}), \qquad C^*(0) = 1 \tag{14}$$

where $C^* = C/C_{AA}$ and $0 \leq x^* \leq 1$. The dimensionless parameters F, A_1, and A_2 are defined as follows:

$$F = \frac{K_f\overline{\Delta P}}{GPF} \tag{15}$$

$$A_1 = \frac{a_1C_{AA}}{\overline{\Delta P}} \tag{16}$$

$$A_2 = \frac{a_2{C_{AA}}^2}{\overline{\Delta P}} \tag{17}$$

where $a_1 = 1.629$ mm Hg/(g/100 ml) and $a_2 = 0.2935$ mm Hg/(g/100 ml)^2 for protein concentrations in the range $4 \leq C \leq 10$ g/100 ml. Note that $C^*(1) = C_{EA}/C_{AA}$. The solution to equation 14 is:

$$\frac{A_1}{2} \ln \left| \frac{C^{*2}}{1 - A_1C^* - A_2C^{*2}} \right| - \frac{1}{C^*} + \left(\frac{A_1^2 + 2A_2}{2\sqrt{A_1^2 + 4A_2}} \right) \times \ln \left| \frac{\sqrt{A_1^2 + 4A_2} + A_1 + 2A_2C^*}{\sqrt{A_1^2 + 4A_2} - A_1 - 2A_2C^*} \right| = Fx^* + I \tag{18}$$

where I is an integration constant determined by the initial condition, $C^*(0) = 1$. Equation 18 provides a means to determine F from the measured values of C_{AA}, $\overline{\Delta P}$, and $C^*(1)$. K_f is then calculated from F, $\overline{\Delta P}$, and GPF, according to equation 15.

RESULTS

The measured determinants of glomerular ultrafiltration in plasma loaded rats are summarized in Table I. Before changes in renal perfusion pressure induced either by aortic constriction or carotid occlusion, SNGFR averaged 49.6 nl/min and GPF 201 nl/min. When $\overline{\Delta P}$ was decreased by aortic constriction, SNGFR and GPF fell significantly, on average to 42.6 and 173

[3] The use of this equation assumes the axial variation in P_{GC} to be negligible. The justification for this assumption is discussed elsewhere (1).

TABLE I

A Summary of the Measured Determinants of Glomerular Ultrafiltration

Condition	$\overline{\Delta P}$	$\bar{P}_{GC}$	P_T	P_C	C_{AA}	C_{EA}	π_{AA}	π_{EA}	$\frac{\pi_{EA}}{\bar{P}_{GC} - P_T}$	SNGFR	SNFF	GPF
	mm Hg	*mm Hg*	*mm Hg*	*mm Hg*	*g/100 ml*		*mm Hg*	*mm Hg*		*nl/min*		*nl/min*
5% Plasma loading	111.0*	54.6	13.4	11.3	6.5	8.7	22.9	36.7	0.87	49.6	0.25	200.6
	±1.6	0.4	0.2	0.3	0.1	0.1	0.4	0.5	0.01	1.5	0.01	7.4
	(22)‡	(22)	(22)	(22)	(22)	(22)	(22)	(22)	(22)	(22)	(22)	(22)
5% Plasma loading	87.0	50.8	12.3	10.2	6.3	8.4	22.1	34.6	0.89	42.6	0.25	173.0
plus	±1.9	0.6	0.4	0.3	0.1	0.2	0.7	1.2	0.02	3.0	0.01	11.2
aortic constriction	(9)	(9)	(9)	(9)	(8)	(8)	(8)	(8)	(8)	(8)	(8)	(8)
P value	<0.001	<0.001	>0.1	<0.05	<0.01	<0.001	<0.01	<0.001	>0.5	<0.001	>0.5	<0.005
5% Plasma loading	148.0	57.2	13.2	10.5	6.5	8.5	22.9	34.9	0.79	65.3	0.23	309.1
plus	±3.0	1.0	0.3	0.4	0.1	0.2	0.6	1.5	0.03	2.2	0.02	30.7
carotid occlusion	(8)	(8)	(8)	(8)	(8)	(8)	(8)	(8)	(8)	(7)	(8)	(7)
P value§	<0.001	>0.05	>0.1	>0.1	>0.4	>0.4	>0.4	>0.4	<0.025	<0.001	>0.4	<0.025

* Mean±1 SE.

‡ Number in parenthesis denotes n animals.

§ Calculated from paired data in each rat using Student's *t* test.

nl/min, respectively (Table I). Carotid occlusion resulted in parallel and significant increases in SNGFR and GPF, to mean values of 65.3 nl/min and 309 nl/min, respectively. Despite small differences in C_{AA} and C_{EA} among the three conditions, SNFF in each case averaged about 0.25, as compared with the value of 0.33 typically found using the same methods in normal hydropenic rats (1–3).

$\bar{P}_{GC}$ changed in parallel with $\overline{\Delta P}$, but the ratio $\bar{P}_{GC}/\overline{\Delta P}$ was higher during aortic constriction (mean = 0.60±0.01 SE) than during carotid occlusion (0.39±0.01), compared with an average of 0.49±0.01 during control. $\bar{P}_{GC}$ before alterations in $\overline{\Delta P}$ averaged 54.6±0.4 mm Hg (range: 50–58 mm Hg), a value approximately 10 mm Hg greater than that in hydropenic rats (1–3). P_T before alterations in $\overline{\Delta P}$ averaged 13.4±0.2 mm Hg, so that $\overline{\Delta P}$ averaged 41 mm Hg, or some 6 mm Hg greater than in hydropenia (1–3). During aortic constriction and carotid occlusion, $\overline{\Delta P}$ averaged 38 and 44 mm Hg, respectively. P_T and P_C both remained essentially unchanged (Table I). P_{EA} averaged 15.4±0.4 mm Hg during control, 13.2±0.6 during aortic constriction, and 14.5±0.6 during carotid occlusion.

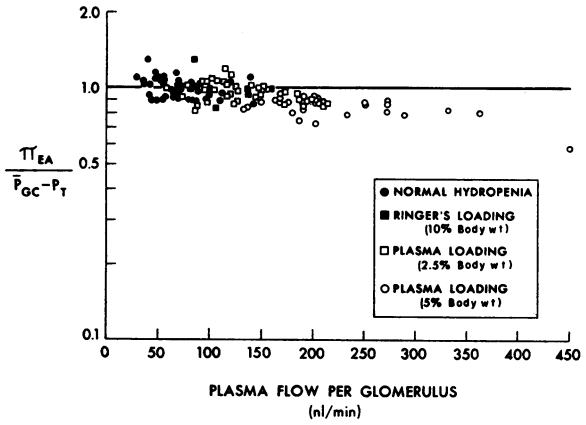

FIGURE 2 Extent of equilibrium as a function of GPF. Symbols denote individual animals. Normal hydropenia, Ringer loading (10% body wt) and plasma loading (2.5% body wt) data are from previous studies (1–3).

An estimate of $\Delta\pi/\Delta P$ at the efferent end of the glomerulus is given by $\pi_{EA}/(\bar{P}_{GC} - P_T)$. Filtration pressure equilibrium exists when this ratio is unity, a condition observed in previous studies (1–4) in which GPF did not reach the very high values induced in the present study. As shown in Table I, $\pi_{EA}/(\bar{P}_{GC} - P_T)$ averaged 0.87±0.01 during control, 0.89±0.02 during aortic constriction, and 0.79±0.03 during carotid occlusion. Thus, the disequilibrium condition required to calculate K_f was satisfied at the high values of GPF obtained in this study. The dependence of $\pi_{EA}/(\bar{P}_{GC} - P_T)$ on GPF is demonstrated in Fig. 2, which shows combined data from individual rats in the present and in previous studies from this laboratory (1–3). For glomerular plasma flows below approximately 150 nl/min, values of $\pi_{EA}/(\bar{P}_{GC} - P_T)$ cluster randomly about 1, indicating (on average) filtration pressure equilibrium. Above 150 nl/min, disequilibrium predominates and $\pi_{EA}/(\bar{P}_{GC} - P_T)$ tends to decrease progressively as plasma flow is increased.

The departures from equilibrium observed in this study are further summarized in Table II. Whereas in previous studies (1–4), P_{UF} has been found to decline essentially to zero by the efferent end of the glomerular capillary, here P_{UF} (denoted by $P_{UF_{EA}}$) declines only

TABLE II

Net Ultrafiltration Pressures at Afferent and Efferent Ends of the Glomerular Capillary

Condition	$\overline{AP}$	$P_{UF_{AA}}$	$P_{UF_{EA}}$
		mm Hg	
5% Plasma loading	111.0*	18.3	5.0
	±1.6	0.5	0.6
	(22)	(22)	(22)
5% Plasma loading plus aortic constriction	87.0	16.5	4.1
	±1.9	0.7	0.6
	(9)	(8)	(8)
P value	<0.001	<0.025	>0.2
5% Plasma loading plus carotid occlusion	148.0	21.1	9.1
	±3.0	1.1	1.5
	(8)	(8)	(8)
P value	<0.001	<0.025	<0.05

* Symbols and terms as defined in Table I.

TABLE III

Ultrafiltration Coefficient as a Function of Glomerular Plasma Flow

Condition	$\overline{AP}$	GPF	K_f
	mm Hg	*nl/min*	*nl/(s·mm Hg)*
5% Plasma loading	111.0	201.0	0.0784
	±1.6	±7.4	±0.0057
	(22)	(22)	(21)*
5% Plasma loading plus aortic constriction	87.0	173.0	0.0772
	±1.9	±11.2	±0.0069
	(9)	(8)	(8)
P value	<0.001	<0.005	>0.2
5% Plasma loading plus carotid occlusion	148.0	309.0	0.0794
	±3.0	±30.7	±0.0054
	(8)	(7)	(7)
P value	<0.001	<0.025	>0.1

* One animal in this group did not fulfill the condition $\pi_{EA}/(\bar{P}_{GC} - P_T) < 1$, so that K_f could not be computed.

to averages of 5.0±0.6 mm Hg during control, 4.1±0.6 mm Hg during aortic constriction, and 9.1±1.5 mm Hg during carotid occlusion.

Calculation of K_f using equations 15 and 18 leads to the results in Table III. As shown, values of K_f were essentially identical in each of the three conditions, despite large and significant differences in GPF. For paired data, changes in K_f averaged −0.001 nl/(s·mm Hg)±0.006 ($P > 0.5$, range: −0.026 to +0.020) following partial aortic constriction and +0.009±0.005 ($P > 0.1$, range: −0.007 to +0.031) following carotid occlusion. As expected, the value of K_f obtained here, about 0.08 nl/(s·mm Hg), is greater (by 33%) than that recently reported for normal hydropenic rats (3), in that the previous calculation assumed $\bar{\pi}_{GC} = (\pi_{AA} + \pi_{EA})/2$, which systematically overestimates $\bar{P}_{UF}$ and underestimates K_f (5).

The assumption of zero axial pressure drop inherent in equations 14 and 18 can easily be relaxed to allow for small decreases in ΔP with x. K_f is then calculated numerically from a more general form of equation 14 (5, 18). When these small axial pressure drops are allowed, the effect on K_f is negligible. For example, assuming an axial pressure drop of 2 mm Hg rather than zero increases the mean K_f by only 3% for control, 4% for aortic constriction, and 1% for carotid occlusion. As noted elsewhere, larger axial pressure drops are not consistent with experimental findings (1).

TABLE IV

Summary of Blood Flows and Resistances across Single Afferent and Efferent Arterioles

Condition	$\overline{AP}$	GBF	EABF	R_A	R_E	R_{TA}	$\frac{R_A}{R_{TA}}$	$\frac{R_E}{R_{TA}}$
	mm Hg	*nl/min*	*nl/min*		10^{10} *dyn·s·cm*$^{-5}$			
5% Plasma loading	111.0*	308.0	259.0	1.5	1.4	2.9	0.52	0.48
	±1.6	11.9	11.1	0.1	0.1	0.1	0.01	0.01
	(22)	(22)	(22)	(22)	(22)	(22)	(22)	(22)
5% Plasma loading plus aortic constriction	87.0	269.0	227.0	1.0	1.5	2.5	0.42	0.58
	±1.9	20.2	18.2	0.1	0.1	0.2	0.01	0.01
	(9)	(8)	(8)	(8)	(8)	(8)	(8)	(8)
P value	<0.001	<0.01	<0.01	<0.001	<0.025	>0.2	<0.001	<0.001
5% Plasma loading plus carotid occlusion	148.0	460.0	395.0	1.6	1.0	2.6	0.62	0.38
	±3.0	39.5	38.8	0.2	0.1	0.3	0.01	0.01
	(8)	(7)	(7)	(7)	(7)	(7)	(7)	(7)
P value	<0.001	<0.025	<0.025	>0.5	<0.025	>0.2	<0.005	<0.005

* Symbols and terms as defined in Table I.

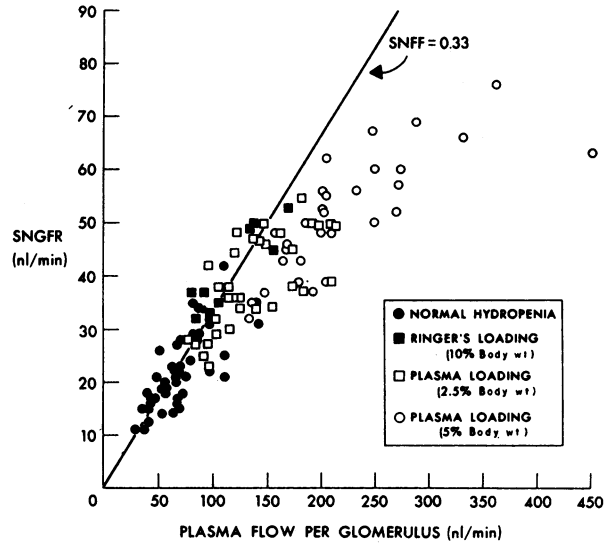

FIGURE 3 SNGFR as a function of GPF rate. Symbols denote individual animals. Normal hydropenia, Ringer loading (10% body wt), and plasma loading (2.5% body wt) data are from previous studies (1–3).

The pressures and flows measured in this study also permit calculation of resistance to blood flow in single afferent and efferent arterioles, the results of which are summarized in Table IV. The fraction of total arteriolar resistance contributed by the afferent arteriole (R_A/R_{TA}) tended to increase, and therefore the fraction of the total contributed by the efferent arteriole (R_E/R_{TA}) decreased, with increasing GBF.

DISCUSSION

The experimental aim of this study was to examine glomerular dynamics under conditions in which filtration pressure equilibrium is not achieved. Disequilibrium, obtained at the elevated glomerular plasma flow rates found during 5% plasma loading, is required to obtain a physically meaningful estimate of the ultrafiltration coefficient, K_f. In addition, the present study was designed to investigate whether K_f is dependent on GPF. This was accomplished by either further increasing GPF (carotid occlusion and vagotomy) or modestly decreasing GPF (partial aortic constriction), always within a range of GPF in which disequilibrium persisted.

Previous studies under equilibrium conditions (1, 2) have shown that SNGFR can be highly plasma-flow dependent. The present results demonstrate that SNGFR remains flow dependent during disequilibrium, but the degree of flow dependence decreases progressively with increasing GPF. This relationship is illustrated in Fig. 3, based on data obtained in this and previous studies (1–3) from this laboratory. Below glomerular plasma flow rates of about 150 nl/min (approximately twice the mean value for normal hydropenia), SNGFR increases in proportion to GPF. As indicated by the straight line in Fig. 3, filtration fraction (SNFF) remains constant at about 0.33 over this range of GPF. However, SNFF declines as GPF increases, as evidenced by the distribution of data points uniformly below the SNFF = 0.33 line for GPF > 150 nl/min. At the very high plasma flows achieved in the present study, SNFF $\cong$ 0.25.

Inspection of equation 2 indicates that the mechanism whereby SNGFR changes in parallel with GPF may involve flow-induced changes either in K_f, $\bar{P}_{UF}$, or both. Recent studies (1, 2), which examined glomerular dynamics at plasma flows ranging from about two-thirds to twice normal (at equilibrium), have led us to reason that whereas a mechanism primarily involving flow-induced changes in $\bar{P}_{UF}$ seemed the simplest and therefore most attractive possibility, flow-induced changes in K_f could not be excluded, since at equilibrium only the product of K_f and $\bar{P}_{UF}$ is known. In the present study, where disequilibrium allows K_f and $\bar{P}_{UF}$ to be calculated independently, we find K_f to be essentially constant over a very wide range of GPF. Accordingly, under these conditions, the observed flow-induced changes in SNGFR are mediated almost exclusively by changes in $\bar{P}_{UF}$.

Whereas the present data cannot be taken as proof that K_f is independent of GPF at the lower flow rates which typically yield equilibrium (GPF < ~150

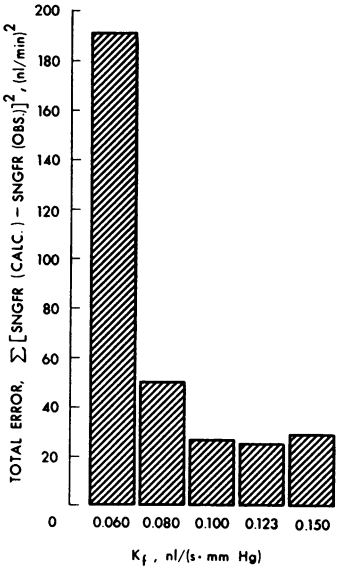

FIGURE 4 Error in simulating previously observed (1–3) values of SNGFR as a function of ultrafiltration coefficient, K_f. These studies (1–3) were characterized by filtration pressure equilibrium.

TABLE V

*Comparison of Calculated and Observed SNGFR**
K_f = 0.10 and 0.08 nl/(s·mm Hg)

Condition	GPF (obs.)	SNGFR (obs.)	SNGFR (calc., K_f = 0.10‡)	SNGFR (calc., K_f = 0.08‡)
		nl/min		
Normal hydropenia§	80.0	27.6±3.6 SE	28.5	28.4
Normal hydropenia‖	65.0	20.5±1.3	20.5	20.4
2.5% Plasma loading	131.0	39.5±3.0	36.8	35.2
10% Ringer loading	111.0	39.5±2.5	38.0	35.8
Normal hydropenia¶				
Preconstriction	80.3	26.8±2.5	28.1	27.9
Aortic constriction	77.5	24.1±2.4	24.6	24.3
Aortic constriction	69.6	18.6±2.1	19.2	18.7
Aortic constriction	50.6	9.0±1.1	11.6	11.0
2.5% Plasma loading¶				
Preconstriction	145.0	40.3±2.1	40.2	37.8
Aortic constriction	124.0	34.0±2.3	34.1	32.5
Aortic constriction	100.0	25.6±2.4	28.3	27.4

* obs. = observed, calc. = calculated.
‡ K_f is in units of nl/(s·mm Hg).
§ Reference 3.
‖ Reference 1.
¶ Reference 2.

nl/min), it is possible to determine whether the present value of K_f, 0.08 nl/(s·mm Hg), is consistent with data obtained at these lower flow rates. A recently described model of glomerular ultrafiltration in the rat (5) has already been employed to simulate the changes in SNGFR found during volume expansion or aortic constriction (1, 2), using a value of K_f consistent with the finding of filtration equilibrium but otherwise arbitrarily chosen. Since this assumed value of K_f, 0.10 nl/(s·mm Hg), is greater than that found in the present study, 0.08 nl/(s·mm Hg), we undertook to determine whether this lower value of K_f is also compatible with our previous equilibrium data (lower GPF). The model was used, as described previously (1, 2), to calculate SNGFR from mean values of $\overline{\Delta P}$, C_{AA}, and GPF measured under various equilibrium conditions (1–3), using the above K_f values as well as several others. The extent of agreement between these calculated values of SNGFR and values measured under a variety of conditions (1–3) is summarized in Fig. 4. The total error in fitting the observed values of SNGFR was taken as the sum of the squares of the differences between SNGFR (calculated) and SNGFR (observed). K_f = 0.06 nl/(s·mm Hg) is clearly inadequate, and since it was also found to underestimate SNGFR in most cases, lower values of K_f must be even more unsatisfactory. As expected, little improvement is gained by raising K_f above 0.10 nl/(s·mm Hg), in that once equilibrium is reached, further increases in K_f cause $\Delta\pi$ to equal ΔP closer to the afferent end of the glomerular capillary, but do not noticeably alter SNGFR.

According to the error criterion used in Fig. 4, K_f = 0.10 nl/(s·mm Hg) provides a slightly better fit to previous data than K_f = 0.08 nl/(s·mm Hg). However, as shown in Table V, if calculated values of SNGFR for these two choices of K_f are compared with each other and with observed values for SNGFR, there emerges no strong basis for preferring one K_f value over the other. Thus, since the K_f value of 0.08 nl/(s·mm Hg) determined experimentally at high plasma flow rates also satisfies the K_f requirement of previous data (1–3) at much lower plasma flow rates, further support is given to the hypothesis that K_f is largely independent of GPF.

Since $K_f = kS$ (equation 2), the effective hydraulic permeability (k) of the glomerular capillary can be estimated from K_f and the surface area available for ultrafiltration (S). Taking K_f = 0.078 nl/(s·mm Hg) and S = 0.0019 cm² for the rat glomerulus (19), we obtain k = 41 nl/(s·mm Hg·cm²). Based on indirect estimates of glomerular pressures, Pappenheimer, Renkin, and Borrero (20) and Renkin and Gilmore (21) report values of 3.4 and 5.4 nl/(s·mm Hg·cm²),

respectively. From previous direct measurements of glomerular pressures, Brenner, Troy, and Daugharty (3) calculated a minimum value of 31 nl/(s·mm Hg·cm^2) by assuming $\bar{\pi}_{GC} = (\pi_{AA} + \pi_{EA})/2$. Our estimate of k for the rat glomerular capillary is thus even higher than previously reported (3, 20, 21), and is some 50 times greater than that recently found for capillaries in rat skeletal muscle (22).

ACKNOWLEDGMENTS

The authors wish to thank Miss Iris F. Ueki and Miss Carolyn Wong for excellent technical assistance and Miss Meredith Clark for expert secretarial assistance.

These studies were supported in part with funds from the U. S. Public Health Service (AM 13888), Veterans Administration and the Stanford University Research Development Fund.

REFERENCES

1. Brenner, B. M., J. L. Troy, T. M. Daugharty, W. M. Deen, and C. R. Robertson. 1972. Dynamics of glomerular ultrafiltration in the rat. II. Plasma-flow dependence of GFR. *Am. J. Physiol.* **223**: 1184.
2. Robertson, C. R., W. M. Deen, J. L. Troy, and B. M. Brenner. 1972. Dynamics of glomerular ultrafiltration in the rat. III. Hemodynamics and autoregulation. *Am. J. Physiol.* **223**: 1191.
3. Brenner, B. M., J. L. Troy, and T. M. Daugharty. 1971. The dynamics of glomerular ultrafiltration in the rat. *J. Clin. Invest.* **50**: 1776.
4. Andreucci, V. E., J. Herrera-Acosta, F. C. Rector, Jr., and D. W. Seldin. 1971. Effective glomerular filtration pressure and single nephron filtration rate during hydropenia, elevated ureteral pressure, and acute volume expansion with isotonic saline. *J. Clin. Invest.* **50**: 2230.
5. Deen, W. M., C. R. Robertson, and B. M. Brenner. 1972. A model of glomerular ultrafiltration in the rat. *Am. J. Physiol.* **223**: 1178.
6. Brenner, B. M., K. H. Falchuk, R. I. Keimowitz, and R. W. Berliner. 1969. The relationship between peritubular capillary protein concentration and fluid reabsorption by the renal proximal tubule. *J. Clin. Invest.* **48**: 1519.
7. Brenner, B. M., and J. H. Galla. 1971. Influence of postglomerular hematocrit and protein concentration on rat nephron fluid transfer. *Am. J. Physiol.* **220**: 148.
8. Brenner, B. M., J. L. Troy, and T. M. Daugharty. 1972. Pressures in cortical structures of the rat kidney. *Am. J. Physiol.* **222**: 246.
9. Brenner, B. M., T. M. Daugharty, I. F. Ueki, and J. L. Troy. 1971. The quantitative assessment of proximal tubule function in single nephrons of the rat kidney. *Am. J. Physiol.* **220**: 2058.
10. Falchuk, K. H., and R. W. Berliner. 1971. Hydrostatic pressures in peritubular capillaries and tubules in the rat kidney. *Am. J. Physiol.* **220**: 1422.
11. Wiederhielm, C. A., J. W. Woodbury, S. Kirk, and R. F. Rushmer. 1964. Pulsatile pressures in the microcirculation of frog's mesentery. *Am. J. Physiol.* **207**: 173.
12. Landis, E. M., and J. R. Pappenheimer. 1963. Exchange of substances through the capillary walls. *Handb. Physiol. Circulation.* **2**: 961.
13. Brenner, B. M., I. F. Ueki, and T. M. Daugharty. 1972. On estimating colloid osmotic pressure in pre- and postglomerular plasma in the rat. *Kidney Int.* **2**: 51.
14. Brenner, B. M., C. M. Bennett, and R. W. Berliner. 1968. The relationship between glomerular filtration rate and sodium reabsorption by the proximal tubule of the rat nephron. *J. Clin. Invest.* **47**: 1358.
15. Vurek, G. G., and S. E. Pegram. 1966. Fluorometric method for the determination of nanogram quantities of inulin. *Anal. Biochem.* **16**: 409.
16. Führ, J., J. Kaczmarczyk, and C. D. Krüttgen. 1955. Eine einfache colorimetrische methode zur inulinbestimmung für nieren-clearanceuntersuchungen bei stoffwechselgesunden und diabetikern. *Klin. Wochenschr.* **33**: 729.
17. Lowry, O. H., N. J. Rosebrough, A. L. Farr, and R. J. Randall. 1951. Protein measurement with the Folin phenol reagent. *J. Biol. Chem.* **193**: 265.
18. Deen, W. M., C. R. Robertson, and B. M. Brenner. 1973. A model of peritubular capillary control of isotonic fluid reabsorption by the renal proximal tubule. *Biophys. J.* **13**: 340.
19. Kirkman, H., and R. E. Stowell. 1942. Renal filtration surface in the albino rat. *Anat. Rec.* **82**: 373.
20. Pappenheimer, J. R., E. M. Renkin, and L. M. Borrero. 1951. Filtration, diffusion, and molecular sieving through peripheral capillary membranes. A contribution to the pore theory of capillary permeability. *Am. J. Physiol.* **167**: 13.
21. Renkin, E. M., and J. P. Gilmore. Glomerular filtration. *Handb. Physiol. Kidney.* In press.
22. Smaje, L., B. W. Zweifach, and M. Intaglietta. 1970. Micropressures and capillary filtration coefficients in single vessels of the cremaster muscle in the rat. *Microvasc. Res.* **2**: 96.